GEOLOGICA CARPATHICA, FEBRUARY 2021, 72, 1, 68–81 https://doi.org/10.31577/GeolCarp.72.1.5

Specific green zonal silica nodules of serpentinite weathering: Unusual products of silicification in laterite-like residuum (Moldanubian Zone, Bohemian Massif)

ŠÁRKA KONÍČKOVÁ[1, ✉], ZDENĚK LOSOS[1], STANISLAV HOUZAR[2] and DALIBOR VŠIANSKÝ[1]

[1]Department of Geological Sciences, Faculty of Science, Masaryk University, Kotlářská 2, 611 37, Brno, Czech Republic;
✉327669@mail.muni.cz, losos@sci.muni.cz
[2]Department of Mineralogy and Petrography, Moravian Museum, Zelný trh 6, 659 37, Brno, Czech Republic

(Manuscript received April 17, 2020; accepted in revised form December 14, 2020; Associate Editor: Peter Bačík)

Abstract: Massive quartz–*chalcedony*±opal nodules ("plasma" in gemology) represent a specific silica variety, which occurs in the laterite-like residues of pre-Miocene paleo-weathering of ultramafites in western Moravia (Moldanubian Zone, Bohemian Massif). These zonal silica nodules (ZSN) tend to have concentric texture with a dark green to green-brown core, pale green margin and a narrow white rim (outer surface zone). The most typical microscopic feature of ZSN is vermiform microstructure particularly in the two outer zones. Individual zones consist of micro- to non-crystalline SiO_2 polymorphs with variable contents of H_2O (quartz, *chalcedony*, moganite, opal-C/CT and opal-A). The predominant green colour is due to submicroscopic smectite pigment, while the brownish colour originated from decomposition of smectite to iron oxohydroxides. ZSN formed in subaerial, partially reducing conditions in the lower part of weathering crusts covering serpentinites. The whole process was preceded by component exchange (chloritization) along serpentinite –felsic rocks (granulite, migmatite, pegmatite veins) boundaries. The gradual silica migration and subsequent redistribution associated with the removal of aluminium, magnesium and iron led up to the formation of a zonal nodular texture dominated by SiO_2 polymorphs. Newly formed minerals in micro-cavities and cracks of ZSN are represented by accessory pyrite and sporadic barite. Zonal silica nodules-bearing residues on serpentinites occur only in a narrow area which was originally covered by clay-sandy Miocene sediments of the Carpathian Foredeep in western Moravia. Probably late low-temperature fluid interaction between silicified serpentinite residuum (chlorite–montmorillonite saprolite) and marine sediments may be the main factor controlling formation of ZSN.

Keywords: Bohemian Massif, Carpathian Foredeep, paleo-weathering, Miocene sediment–serpentinite interaction, green zonal silica nodule.

Introduction

Weathering of ultrabasic rocks (dunite, peridotite, serpentinite) produces due to their instability during tropical and subtropical conditions variable silicified clay residua, which contain SiO_2-rich materials, especially microcrystalline and fibrous quartz, moganite and opals (Rice & Cleveland 1955; Venturelli et al. 1997; Lacinska & Styles 2013; Ulrich et al. 2014).

One of these silica varieties, which are formed in strongly weathered serpentinites is specific green-brownish zonal silica fragments, referred to as "plasma" in gemology (Hurlbut & Kammerling 1991). It is typically formed by various micro- to non-crystalline SiO_2 polymorphs with variable contents of H_2O, especially quartz, *chalcedony* (mixture of fibrous quartz), moganite and opal-C/CT (Heaney et al. 1994; Chauviré et al. 2017). The unique deep green zonal "plasma" (ZSN – zonal silica nodules in this paper is used) occurs only in the specific conditions and in the narrow restricted area of serpentinite residues in western Moravia (Mrázek & Rejl 2010; Koníčková 2014, 2015).

The aim of this research is to specify the position and possible genetic conditions of ZSN origin by means of a more detailed mineralogical and chemical study and thus clarify their unique occurrence in Central Europe.

Geological background

Ultrabasic rocks enclosed in granulites, orthogneisses and migmatites are part of the Gföhl Unit in the Moldanubian Zone (Bohemian Massif, western Moravia; Fig. 1). Their protoliths include peridotite, dunite and lherzolite, and sporadically also pyroxenite. Most of these ultrabasic rocks were affected by strong hydration – serpentinization; therefore, they contain antigorite, chrysotile or lizardite that predominate over relics of olivine and enstatite, and sporadic Cr-rich spinel, chromite, magnesiochromite, pyrope, diopside and pargasite. On the other hand, younger magnetite and chlorite are locally common. They usually contain intercalations of these felsic rocks and locally are also injected by numerous pegmatite veins affected by desilicification. These rocks are often completely chloritized; chloritization also resulted in occurrence of relatively common veins of chlorite sometimes accompanied by anthophyllite and/or tremolite (Rejl et al. 1982; Medaris et al. 2005; Novák 2005).

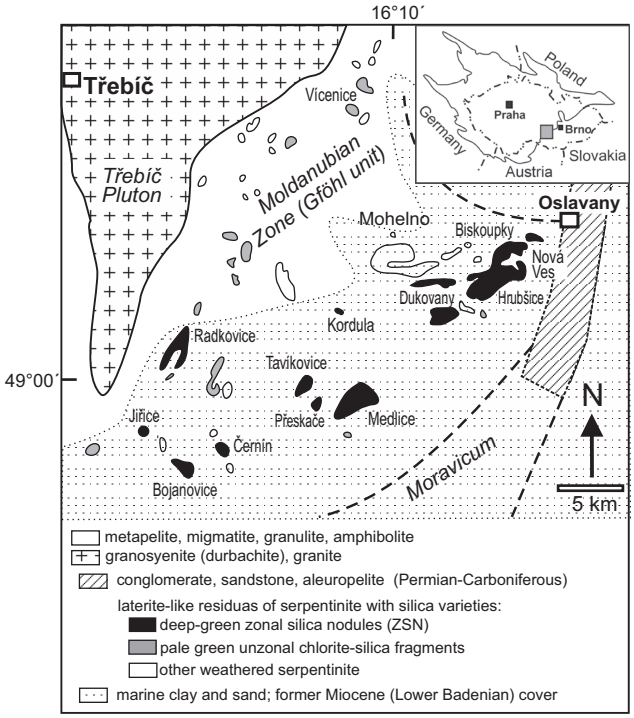

Fig. 1. Geological situation of ZSN-bearing lateritic-like residues on serpentinites and other ultrabasic bodies in south-western Moravia (modified after Koníčková 2014).

The thickness of the weathering crust that formed in the warm and humid tropical to subtropical climate on top of serpentinite bodies reached up to 30 metres. However, complete profiles of nickel-bearing deep laterite-like bodies (only sporadic aluminum hydroxides are present) are rarely preserved (Kudělásek et al. 1972).

The top part of residues contains (due to subsequent erosion only locally) goethite, hematite, maghemite, magnetite, nontronite, metahalloysite-chlorite, and sporadic gibbsite ("red weathering zone", with Ni<0.7 wt. %). The chemistry of the underlying zone of "green weathering" is markedly chemically affected by the gneiss relics. This zone contains abundant Ni-montmorillonite, Ni-nontronite and "Ni-chlorite" (1–4 wt. % Ni). Remnants from felsic rocks include quartz, K-feldspar, almandine and zircon. The lowest zone of "grey weathering" is characterized by numerous fragments of weathered serpentinite with carbonate coatings and hematite. This zone also has a high content of different varieties of siliceous matter. Clay minerals are represented by nontronite. The base of this zone is very poor in Ni (0–0.5 wt. %), with common fragments of serpentinite, and contains up to 30 % chlorite (Kudělásek et al. 1972; Mátl 1972).

The age of formation of the weathering products is not known precisely but in the studied area of the Bohemian Massif they undoubtedly existed before the transgression of the Lower Miocene sea (Mátl 1972; Dlabač 1976; Francírek & Nehyba 2016; Kováč et al. 2018). Parts of the residual rocks were originally covered by brackish and marine sand-clay sediments (Eggenburgian and Ottnangian to Lower Badenian). Their mutual relations have not been studied in detail yet, but the repeated intervention of the Miocene sea transgressions is obvious in the studied area (Kuhlemann 2007; Rasser et al. 2008; Chlupáč et al. 2011). The ZSN-bearing residues are also locally covered by Middle Miocene to Pleistocene moldavite-bearing gravels (moldavite age 14.6 Ma, Buchner et al. 2010) or late Pleistocene loesses (Trnka & Houzar 2002; Nehyba & Hladilová 2004).

Sample material and experimental methods

In the studied area, two green silica varieties commonly occur as loose rounded fragments in agricultural fields: (a) common unzonal pale green chlorite-bearing silica fragments, and (b) dark green zonal silica nodules (ZSN). They were studied in this paper in detail, and were distinguished by Koníčková (2014). From the number of individual serpentinite bodies in western Moravia where the weathering profiles were developed, typical ZSN are only found in a limited area around Oslavany, Dukovany, Tavíkovice, Bojanovice, Přeskače and Jiřice near Moravské Budějovice (Fig. 1).

Thin sections from representative ZSN were studied using NU-2 Carl Zeiss Jena and Olympus BX41 optical microscopes in transmitted and reflected light and documented by the Canon EOS 1100D digital camera.

Microprobe analyses were carried out at the Joint Laboratory of Electron Microscopy and Microanalysis of the Department of Geological Sciences, Masaryk University and Czech Geological Survey, Brno (analysts P. Gadas, R. Čopjaková) using the Cameca SX 100 microprobe. Measurement was carried out under the following conditions: wavelength dispersion mode, accelerating voltage 15 kV, beam current 10 nA and 20 nA, beam size 2–4 μm. The following standards were used for the analysis of individual oxides and silicates: albite (Na); sanidine (Si, Al, K); wollastonite, grossular (Ca); spessartine (Si, Mn); titanite TiO (Ti); almandine, pyrope, hematite (Fe); topaz (F); chromium (Cr); gahnite (Zn); Mn_2SiO_4 (Mn); $ScVO_4$ (V); barite (Ba); vanadinite (Cl); Ni_2SiO_4 (Ni); $MgAl_2O_4$ (Mg, Al); fluorapatite (P, Ca); $SrSO_4$ (Sr, S); zirconium (Zr). The analytical data were corrected by the PAP routine (Pouchou & Pichoir 1985).

Trace element analysis was performed by laser-ablation inductively coupled plasma mass spectroscopy ***(LA-ICP-MS)*** in the laboratory of the Department of Chemistry, Masaryk University (analyst M. Holá). The instrumentation consisted of LSX-213 G2+laser ablation device (Teledyne Cetac Technologies, USA) and Agilent 7900 ICP-MS analyser (Agilent Technologies, Japan). The laser operates at a wavelength of 213 nm with pulse duration ~4 ns. Using helium as a carrier gas with a flow rate of 0.9 l min^{-1}, the aerosol was washed out of the chamber (HelEx) and transported to the ICP-MS. Analyses were performed as spot ablation using 100 μm of spot diameter, laser fluence of 15 J cm^{-2} and repetition

rate of 10 Hz. The ablation time of one analysis was 60 s. The following isotopes were monitored during the LA-ICP-MS scan measurements: ^{11}B, ^{23}Na, ^{24}Mg, ^{27}Al, ^{29}Si, ^{31}P, ^{34}S, ^{39}K, ^{43}Ca, ^{47}Ti, ^{51}V, ^{52}Cr, ^{55}Mn, ^{57}Fe, ^{59}Co, ^{60}Ni, ^{88}Sr, ^{137}Ba. Integration time was 2.1 s. External calibration was performed using the standard reference materials (SRM) – NIST 610 and NIST 612. Quantification was based on the sum of oxides equal to 100 wt. %.

X-ray powder diffraction

Three zones of a typical ZSN sample from the locality Přeskače were mechanically separated and analysed individually: dark core, pale green margin and white outer surface zone. The samples were ground under isopropyl alcohol using a McCrone Micronizing Mill. In addition, the dark core sample was mixed with 10 wt. % of fluorite used as an internal standard to quantify the amorphous phase content. An oriented mount of the white outer surface zone was prepared on a zero-background silicon monocrystal wafer and saturated with ethylene glycol vapour to prove the presence of smectite. Limited amounts of the samples did not allow the separation of <2 μm fraction. Therefore, the study was conducted on a pulverized bulk sample. Powder X-ray diffraction (PXRD) analysis was conducted at the Department of Geological Sciences at Masaryk University (analyst D. Všianský) using an X'Pert PRO MPD diffractometer, equipped with a Co tube ($\lambda K\alpha$=0.17903 nm), operated at 40 kV and 30 mA, and a 1-D RMTS (real time multiple strip) detector at the Bragg-Brentano parafocusing θ–θ reflection geometry. Step size: 0.033 °2θ, time per step: 160 s, angular range: 5–100 °2θ, which produces the total scan duration of 3684 s. The data obtained were processed using the Panalytical HighScore 3 plus and ICSD 2012 structure models. Quantitative phase analysis was done using the Rietveld method. For moganite, ICSD 2012, reference pattern (structure model) no. 98-006-7669 was used.

Raman spectra

Raman spectra of the SiO_2 phases and accessory minerals were measured by a HORIBA LabRam HR microspectrometer with Si-based Peltier-cooled CCD detector at the Department of Geological Sciences, Masaryk University (analyst Z. Losos and Š. Koníčková). Spectra were evaluated using the LabSpec 6 and PeakFit 4 software. Measuring conditions: red laser 633 nm, green laser 532 nm, room temperature, confocal mode, lens magnification 100× and 50×, grid 600, filter 25–100 %, loading length 2×5 to 2×80 s, range 80–2000 cm^{1}. For each ZSN sample, at least 20 points were measured on the cross-section.

Whole-rock analyses

Samples weighing 10–20 g were used for whole-rock chemical analyses; they were acquired at the Bureau Veritas Laboratories (Vancouver, Canada). Loss on ignition (LOI) was calculated from the weight difference after ignition at 1000 ºC. The rare earth and other trace elements were analysed by ICP-MS following $LiBO_2$ fusion (analytic code: A4B4 – major oxides, Ba, Be, Co, Cr, Cs, Ga, Hf, Nb, Ni, Rb, Sc, Sr, Ta, Th, U, V, W, Y, Zr, REE; 1DX – Ag, As, Au, Bi, Cd, Cu, Hg, Mo, Ni, Pb, Sb, Se, Tl, Zn; 2ALeco – C_{tot}, S_{tot}; for analytical details, reproducibility, and detection limits see http://bureauveritas.com/um).

Results

Mineralogy, zonal texture and vermiform microstructure

The typical ZSN are bluish green to dark green oval nodules with an irregular surface. The nodules are concentric zoned, with a dark green to brown-green translucent core, a pale greenish margin, and a white outer surface zone (rim) (Figs. 2, 3.)

Some polymorphs and varieties of SiO_2 in ZSN were distinguished by an optical study, X-ray diffraction or Raman spectroscopy. The core of ZSN is formed by fine-grained micro-cryptocrystalline mosaic quartz, which forms grains of size ≤500 μm. It also contains aggregates of fine fibrous radial *chalcedony*, but it is more abundant as a filling of contractile cracks and, in particular, the predominant mineral of young veinlets of up to 1 mm in thickness, irregularly penetrating nodules. Sometimes there is also a zonal microstructure of these fillings with a narrow margin of moganite or *quartzine* (one of the fibrous quartz variety in *chalcedony*) at the edge or a wider zone of chalcedony. The centres are filled by microcrystalline granular quartz. Optically isotropic opal occurs on the narrow outer surface of zonal nodules.

A typical microstructure (and very rarely also macrostructure) of ZSN samples, which distinguishes them from other silica products of ultrabasic rock weathering, is a relic vermiform ("worm-like" or "vermicular") microstructure. It is represented by a form of twisted worm-shaped aggregates, consisting of transversely arranged "fibres" and "strips" (Fig. 4a,b).

The vermiform microstructure of the ZSN is developed mainly in its pale green margin and white outer zone (Figs. 3, 5), where different types of opal were identified in vermiform domains and fibrous silica in the matrix corresponds according to the optical view to *quartzine* or moganite. Towards the margin, the boundary of vermiform structure becomes more distinct, as the white outer surface zone of the nodules, which is often formed by younger opal only. Direct ZSN transitions to serpentinites were not found.

Porous, sharply bound areas in homogeneous mass of cores of some ZSN correspond to vermiforms in terms of shape and size. They are formed by coarser crystalline quartz aggregates, which could result from recrystallization of opal with simultaneous reduction of volume leading to formation of pores (Fig. 6).

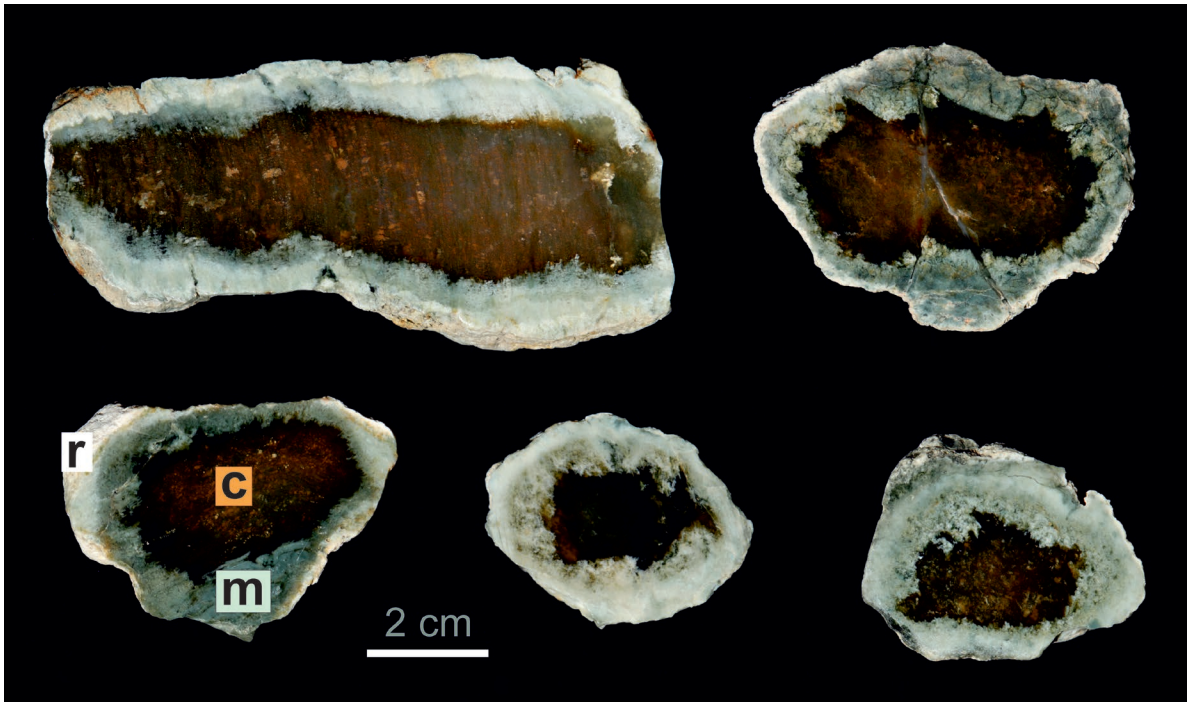

Fig. 2. Typical ZSN from the locality Přeskače with three different zones – dark green to brown core (c), pale green margin (m), white rim (r) (outer surface zone). In the dark core, originally green smectite was partly altered to goethite (photo by D. Všianský).

Mineralogy

Relic minerals of serpentinite

The only microscopically visible relic minerals from the primary rock (serpentinite) are present in ZSN in an accessory amount ≤0.5 vol. %; they are slightly more abundant in the outer parts of the nodules. The most common relic mineral is clinochlore (with 9.37–20.42 wt. % FeO, 0.02–0.69 wt. % Cr_2O_3 and 0.22–1.18 wt. % NiO); it forms sporadic flakes and microcrystalline aggregates. Only colourless amphiboles (magnesio-hornblende, tremolite, pargasite, rarely anthophyllite) are present in addition. From pyroxenes only diopside was determined whereas orthopyroxene (enstatite) which was originally abundant in non-weathered serpentinites was not found. Rare accessory minerals include Cr-rich spinel, chromite, titanite, zircon and Mg-ilmenite (Koníčková 2014; Koníčková et al. 2015).

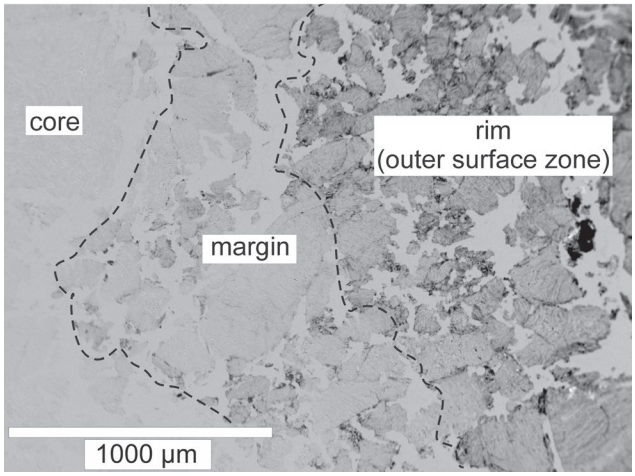

Fig. 3. Profile across ZSN from core to outer surface zone. Light mineral in outer surface zone – late opal. Locality Dukovany, BSE image (photo by P. Gadas).

Minerals of paleo-weathering and silicification

The dominant newly formed minerals of ZSN bound to the palaeo-weathering of serpentinites and silicification of the decomposition products are SiO_2 polymorphs; they comprise about 99.8 vol. % of the nodule material. The most common mineral is microcrystalline quartz, mostly mixed with moganite. Pigment of various Fe, Mg, Al minerals (clay minerals, relic chlorite and serpentine group minerals) is presented in ZSN only in accessory amounts and is responsible for colouring of nodules. In the darkest matrix, these silicates could not be distinguished using an electron microscope, so it can be assumed that main colouring agents already belong to the category of clay minerals (grain size <2 µm).

Based on the association of regularly distributed elements (Si–Mg–Fe–Al) only, the colouring components are probably very finely dispersed phyllosilicates, especially smectites or chlorites. However, powder X-ray diffraction and Raman spectroscopy identified SiO_2 polymorphs and varieties and rare admixture of smectite only (Koníčková 2014; Koníčková et al. 2015).

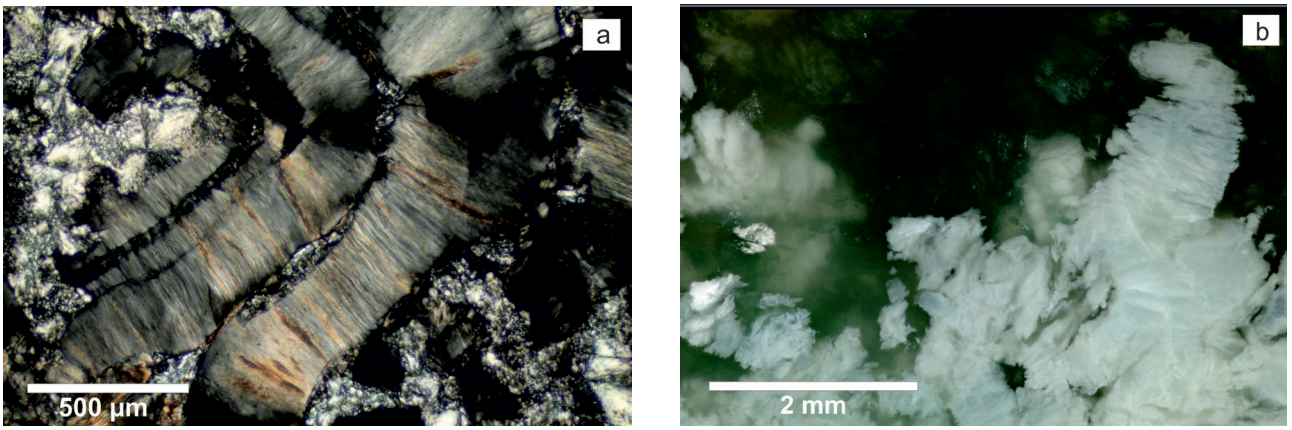

Fig. 4. Typical vermiform ("worm-shaped") microstructures of ZSN margin: **a** — XPL, width 2 mm, photo by Š. Koníčková; **b** — width 5,7 mm, photo by R. Kummer.

X-ray powder diffraction

The X-ray diffraction patterns of the typical silica nodule zones are shown on Fig. 7. The green brown core of the ZSN is dominantly composed of quartz and moganite; since the diffraction pattern of *chalcedony* (i.e. mixture of fibrous quartz and moganite) is identical with that of quartz, optical examination of the sample was necessary to specify that the zone consists of a mixture of quartz and *chalcedony*. The moganite reflection 4.456 Å (4.438 Å according to the database data used – ICSD 2012, reference pattern no. 98-006-7669) appears at 23.255 degrees 2Θ. Moganite (ca. 7 wt. %) and amphibole are present in small amounts; due to their very low content (less than 1 wt. %), the exact amphibole species cannot be assigned based on PXRD data. The content of opal-A (X-ray amorphous phase) reaches ca. 7 wt. %.

The pale green margin is composed of two main phases – granular quartz and microcrystalline opal. It is not clear whether the structure corresponds to opal-C or CT according to its strongest reflection. Cristobalite superstructure weak reflections (Graetsch 1994) are present, but two of them overlap with moganite reflections in the core. This leads to the conclusion that the zone material corresponds partly to opal-C and partly to opal-CT. A small amount of amphibole is present here, as well as in the dark core. Amphibole causes the pale green colour of this zone. Presence of amphibole in ZSN is described in literature, as in Graetsch (1994).

The white outer surface zone (rim) is dominated by opal, minor quartz (chalcedony) and smectite. The opal structure is the same as in the pale green margin. A very weak (0 0 1) reflection of smectite is present in the X-ray diffractogram. After the ethylene glycol solvation, the peak maximum shifted from 14.2 Å to ca. 17.0 Å, which is the evidence of the expandable clay mineral structure presence (Fig. 8).

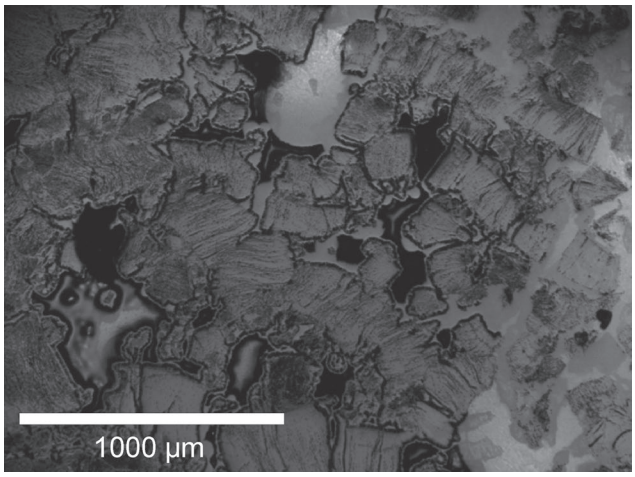

Fig. 5. Vermiform domains in outer surface zone of ZSN replaced and cemented by opal. Reflected light, PPL; photo by Š. Koníčková.

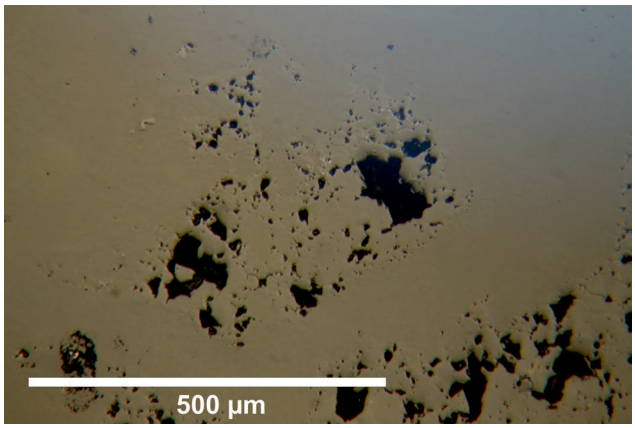

Fig. 6. Quartz aggregates, which could result from recrystallization of opal with simultaneous reduction of volume leading to formation of pores. Reflected light, PPL; photo by Š. Koníčková.

Raman spectra

Using Raman spectroscopy, we examined the gradual transition from (a) fully silicified centre with finely dispersed sub-microscopic inclusions of phyllosilicates ("ghost microstructure") in microcrystalline quartz, to (b) vermiform, completely silicified inhomogeneous aggregates of quartz and

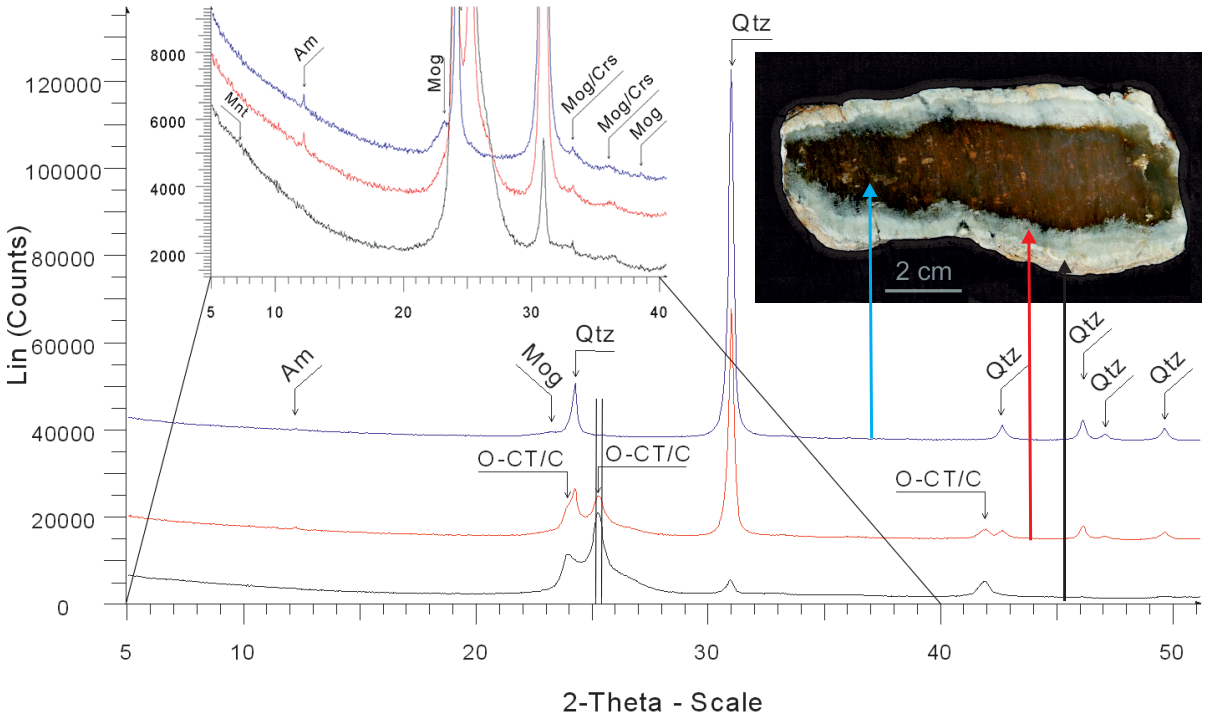

Fig. 7. X-ray powder diffractograms of the three silica nodule zones (locality Přeskače). The vertical lines indicate the difference of the d-spacing in cristobalite (4.04 Å) and tridymite (4.10 Å) (Graetsch 1994). Qtz=quartz, O-CT/C=opal CT/C, Mog=moganite, Am=amphibole, Crs=position of weak superstructure reflections of cristobalite.

chalcedony, and (c) inhomogeneous, opal rich outer zone with clearly-visible vermiform microstructure (Fig. 3).

The dark core of ZSN is homogeneous in reflected light even at high magnification, mostly without recognizable vermiform shapes, but with numerous localized porous areas with dimensions from 0.1 to 1.2 mm. Raman spectra of this mass of core (the same sample from Přeskače as on Fig. 7) correspond to mixture of quartz and moganite (Fig. 9b), as well as in some relicts of vermiform structures. In the porous coarser-grained areas only pure quartz was determined (Fig. 9a); both phases were identified by their most intense Raman bands at 463 cm^{-1} (quartz) and 501 cm^{-1} (moganite) – Kingma & Hemley (1994). Quartz is also characterized by other measured Raman bands (125, 204–205, 261, 352 and 392–394 cm^{-1} (compare to the RRUFF database, http://rruff.info).

The pale green rim is composed of two types of SiO_2 domains: (a) pseudomorphs after phyllosilicates of lower polishing hardness (with a negative relief, partly of vermiform shapes, with lower reflectance) with size ranging from 0.05×0.1 to 0.5×1.8 mm; b) surrounding slightly inhomogeneous mass of higher polishing hardness (with a positive relief and a slightly higher reflectance). Vermiform pseudomorphs correspond to amorphous matter (Raman-inactive opal-A, Fig. 10b), in some samples with significant luminescence under the 532 nm laser. The surrounding harder mass exhibits the typical spectrum of quartz and moganite (Fig. 10a).

The white outer surface of ZSN contains poorly polishable matter which appears as densely accumulated vermiform

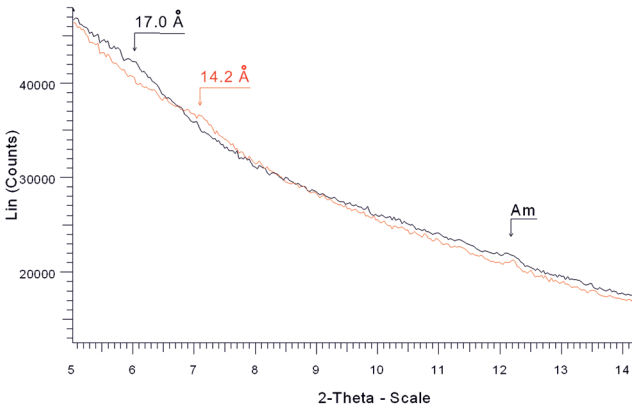

Fig. 8. Comparison of X-ray diffraction patterns of the outer surface zone of ZSN oriented mount before (red line) and after (black line) ethylene glycol solvation; Am=amphibole; weak peaks at 17.0 and 14.2 correspond to smectite.

formations in the reflected light. Its Raman spectra indicate different types of opal (C, CT and amorphous) – the spectrum on Fig. 11b is closely comparable to the reference spectra R060652 (opal C), R060650 (opal CT) or R070627 (Opal C) of the RRUFF database, the wide Raman band between 290 and 350 cm^{-1}, C opal band at ca 415 cm^{-1} and for both types of opal with a sharper peak at the 780 cm^{-1} wavelength. The optically homogeneous, reflective, well-polished younger phase, composed of a mixture of quartz and moganite is present in accessory amount only (Figs. 5, 11a).

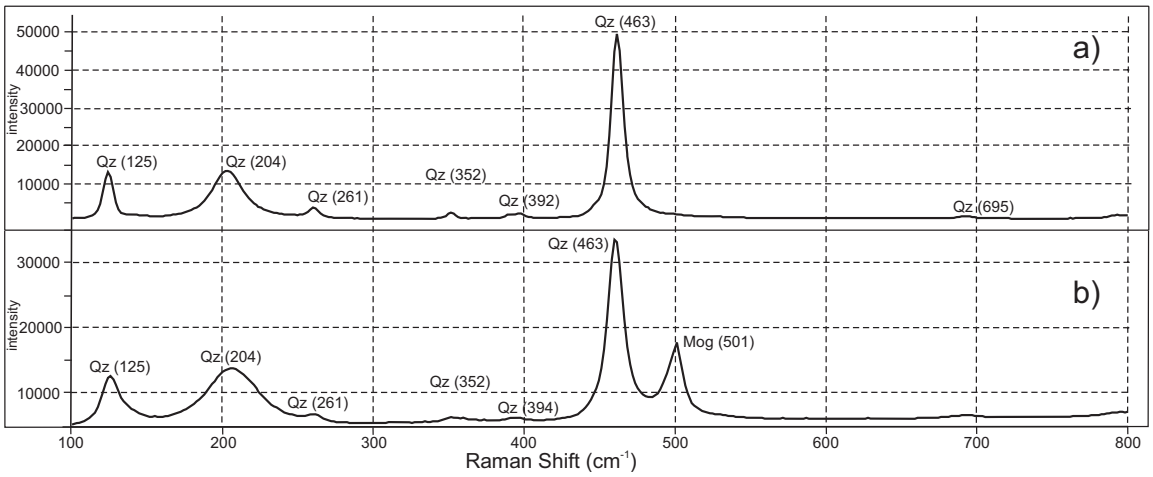

Fig. 9. Raman spectra of the dark core of ZSN: **a** — coarse-grained porous aggregates of quartz (Q); **b** — homogeneous mass composed of quartz (Q) and moganite (M).

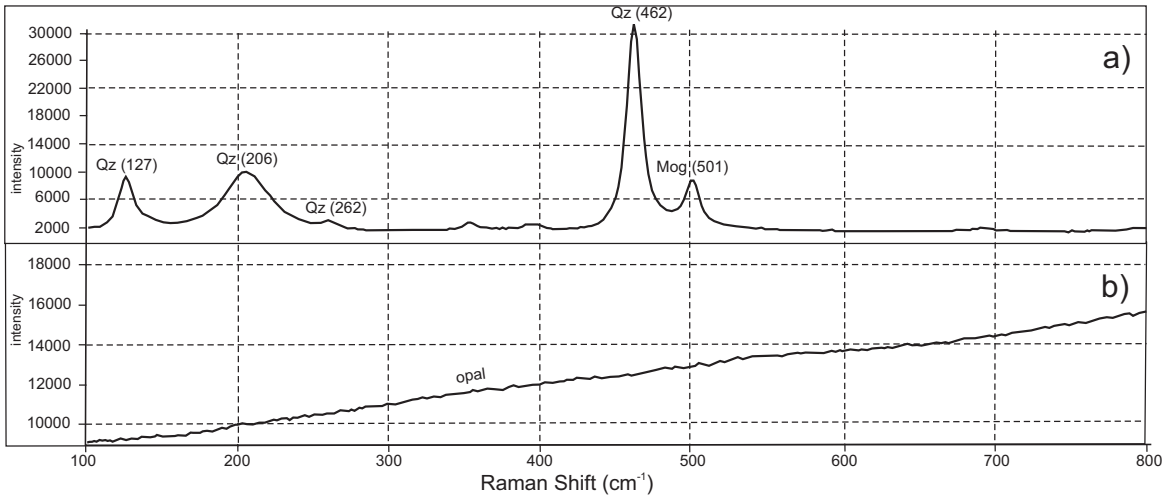

Fig. 10. Raman spectra of the pale green margin of ZSN: **a** — homogeneous domain composed of quartz (Q) and moganite (M); **b** — Raman-inactive opal of softer pseudomorphs after phyllosilicates.

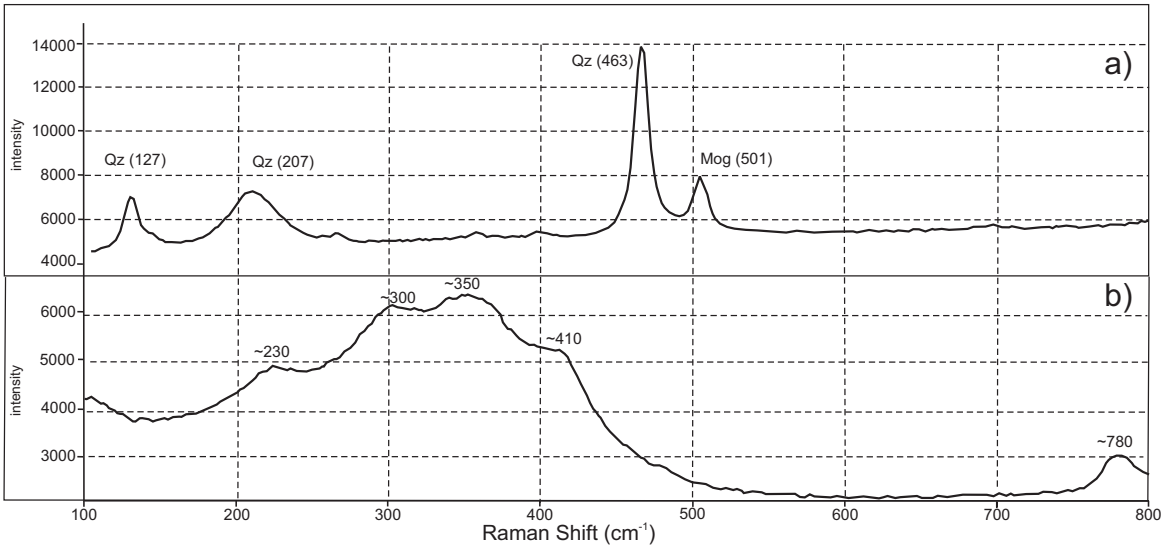

Fig. 11. Raman spectra of the white outer surface zone of ZSN: **a** — homogeneous mass of quartz (Q) and moganite (M); **b** — dominant non-homogeneous less reflecting domain corresponding to opal-C/CT.

Newly formed minerals (pyrite, barite)

The remarkable but rare late-formed accessory mineral of ZSN is pyrite. It forms anhedral grains to euhedral cubic crystals ≤1 mm in size, especially in samples from the vicinity of Dukovany and Jiřice localities. Similar to pyrite, accessory barite (Fig. 12) was locally found in pores and fissures. It occurs in almost all studied samples, in the form of small (<0.2 mm) irregular grains filling small pores or thin cracks together with calcite. Very rare is chlorine-rich "carbonate-apatite" (Koníčková 2014).

Chemical composition

Whole-rock chemistry

The whole-rock (WR) composition of zonal ZSN was studied with in terms of major and trace element components (Table 1). The WR analyses correspond to a strongly silicified residuum dominated by silica (≥94 wt. % SiO_2) and reflects the fact that apart from common quartz and minor moganite, it is composed of fibrous *chalcedony* in core (and margin), abundant opal in outer surface zone, and a very low but variable amount of Mg–Fe–Al phyllosilicates.

The chemical composition of individual zones is variable. From core to outer surface zone, there is an increase of Al_2O_3 (0.10 → 0.31 wt. %), MgO (0.20 → 0.69 wt. %), Ni (21.8 → 130.8 ppm), Co (3.7 → 7.9 wt. %), Cr_2O_3 (0.008 →0.018 wt. %), Rb (<0.1 → 1.7 ppm), Sr (2.6 → 4.7 ppm) and LOI (1.2 → 3.4 wt. %) and decrease of SiO_2 (96.56→ 94.25 wt. %), Fe_2O_3 (1.66 → 0.57 wt. %), Cu (10.6 → 5.2 ppm), Pb (5.1 → 1.0 ppm) and Au (1.2 → 0.5 ppb), which corresponds to the increase of amount of clay minerals (smectites), eventually amphiboles. Highly variable is Ba (9–112 ppm), U (0.1–1.6 ppm), Zr (0.9–13.2 ppm), while contents of CaO and Zn (8–15 ppm) in individual zones vary irregularly. The core also contains slightly elevated Mo, Na and W, whereas Be, Cs, Ga, Hf, Sn, Th, Y, S, and REE are near or below the detection limit. Homogeneous dark green ZSN (locality Hrubšice) contains 924 ppm Ni and 12.1 ppm Co (Koníčková et al. 2015, and this paper).

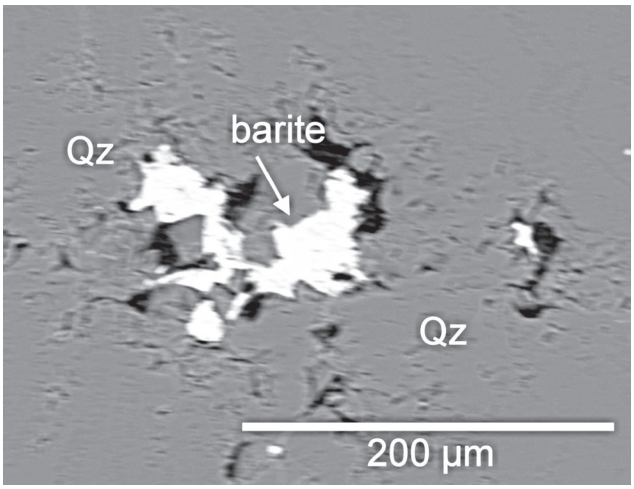

Fig. 12. Barite aggregate filling small cavity in the margin zone of ZSN. BSE image (photo by P. Gadas).

LA-ICP-MS

The dark core of ZSN is characterized by low variability of SiO_2 (98.8–99.6 wt. %) with increased contents of Na (303–446 ppm), K (188–328 ppm), Fe (1173–3511 ppm) and average B (40–71 ppm). Highly variable SiO_2 content (89.3–99.6 wt. %, but often >99 wt. %) is typical in margin zone, similarly to Fe (401–1178 ppm). Contents of other elements are medium compared to cores and outer surface zones. Outer surface zones are slightly poorer in SiO_2 (98.5–98.7 wt. %) and feature the highest contents of Fe (2367–3909 ppm), Ni (139–205 ppm), Cr (332–647 ppm), Ca (420–776 ppm) and Sr (3.24–4.51 ppm), on the contrary B content is below the detection limit (Table 2).

Both Na and K decrease from the core to the outer surface zone while Al, Ca, Mg, Ti, Ni and especially Cr increase. There is a significant positive correlation between Ni, Mg, and Al, and negative one between Si and Al. Occasionally, high contents of Ba (114 and 269 ppm) and in one case also P (28.9 ppm) were found, all in samples with high SiO_2 (>99.5 wt. %); submicroscopic inclusions with low SiO_2 (71.9–90.1 wt.%) rich in Al, Ni, Ca, Sr, Na and Ba were detected locally. Other elements vary in a wide range whereas S and P are usually below the limit of determination.

The distinct variability of elements within SiO_2 grains in the individual zones of ZSN suggests the existence of mineral inclusions a few µm in size rather than presence of these elements in the SiO_2 crystal structure.

Discussion

The main issues that need to be addressed when discussing the origin of the west-Moravian ZSN (zonal green silica nodules="plasma" in gemology) include: (i) mineralogy, shape, zonal texture and presence of vermiform relic microstructures, (ii) regionally very limited occurrence of ZSN and (iii) genesis of zonal silica-rich nodules, which contain clay-sized colouring component (including younger accessory pyrite and barite).

Mineralogy and microstructure

The core of ZSN is composed only of pure silica (grained quartz>>moganite), with randomly disseminated submicroscopic Mg–Fe alumosilicates (smectites) and sporadic chlorite flakes. Maximum of microcrystalline quartz occurs in this zone. In some samples, porous coarser crystalline quartz areas with adsorbed H_2O (<3–5 wt. %) were determined (Koníčková 2014).

Table 1: WR analyses of different zones of ZSN: P1 — core, locality Přeskače; P2+P2 — pale green margin and narrow non-separable outer surface zone (rim), locality Přeskače; NV1a — core, locality Nová Ves; NV1b — margin, locality Nová Ves; NV2 — rim (outer surface zone), locality Nová Ves; H1 — dark green, unzoned, locality Hrubšice; b.d.: Cd, Sb, Bi, Ag, Hg, Tl, Se, Sm, Gd, Eu, Tb, Dy, Ho, Er, Tm, Yb, Lu; total Fe as Fe_2O_3.

Sample		**P1**	**P2+P3**	**NV1a**	**NV1b**	**NV2**	**H1**
		core	margin+rim	core	margin	rim	unzoned (dark)
wt. %	SiO_2	96.18	94.25	96.56	96.23	94.78	95.59
wt. %	P_2O_5	0.02	0.02	0.02	0.02	0.02	0.02
wt. %	TiO_2	<0.01	0.01	<0.01	0.01	<0.01	0.01
wt. %	Al_2O_3	0.10	0.26	0.16	0.22	0.31	0.49
wt. %	Fe_2O_3	1.50	1.22	1.66	0.74	0.57	1.29
wt. %	Cr_2O_3	0.008	0.035	0.013	0.013	0.018	0.010
wt. %	MnO	0.01	<0.01	0.02	<0.01	<0.01	0.01
wt. %	MgO	0.20	0.72	0.22	0.41	0.69	0.81
wt. %	CaO	0.31	0.20	0.10	0.07	0.12	0.08
wt. %	Na_2O	0.04	0.02	0.04	0.03	0.03	0.02
wt. %	K_2O	0.02	0.03	0.02	0.02	0.03	0.02
ppm	Ba	112	48	30	9	44	14
wt. %	LOI	1.6	3.2	1.2	2.2	3.4	1.5
wt. %	Sum	100.02	100.00	100.01	100.00	100.00	100.02
ppm	Be	1	<1	3	<1	<1	<1
ppm	Co	4.6	6.2	3.7	3.9	7.9	12.1
ppm	Cs	<0.1	0.3	<0.1	<0.1	0.3	<0.1
ppm	Ga	<0.5	<0.5	<0.5	<0.5	<0.5	<0.5
ppm	Hf	<0.1	<0.1	<0.1	0.1	<0.1	<0.1
ppm	Nb	0.9	1.0	0.7	0.8	0.7	1.1
ppm	Rb	0.3	1.1	<0.1	0.2	1.7	<0.1
ppm	Sn	<1	1	<1	<1	<1	<1
ppm	Sr	7.5	5.7	2.6	3.7	4.7	2.9
ppm	Th	<0.2	<0.2	<0.2	<0.2	<0.2	<0.2
ppm	U	0.9	0.2	0.1	0.2	0.3	1.6
ppm	V	<8	11	<8	<8	<8	9
ppm	W	1.2	1.1	0.9	0.6	0.6	<0.5
ppm	Zr	5.8	1.3	4.2	13.2	1.6	0.9
ppm	Y	0.1	<0.1	<0.1	<0.1	0.1	<0.1
ppm	La	0.7	0.7	0.3	0.5	0.5	1.2
ppm	Ce	0.2	0.9	0.1	<0.1	<0.1	<0.1
ppm	Pr	<0.02	0.07	<0.02	<0.02	<0.02	<0.02
ppm	Nd	<0.3	0.4	<0.3	<0.3	<0.3	<0.3
ppm	Mo	3.1	2.1	3.5	1.4	1.4	2.1
ppm	Cu	5.2	7.3	10.6	5.7	5.5	6
ppm	Pb	5.1	1	2.9	3.8	2.1	7
ppm	Zn	15	9	8	12	10	25
ppm	Ni	21.8	130.8	29.2	46.6	86	914.2
ppm	As		0.6	1.2			1.3
ppb	Au	0.9	16.3	1.2	0.5	0.5	0.7
%	TOT/C	0.09	0.07	0.03	0.03	0.04	0.03
%	TOT/S	<0.02	<0.02	<0.02	<0.02	<0.02	<0.02

Margins have a typical vermiform microstructure characteristic of nodules, which were partially pseudomorphosed by opal-C/CT and amorphous opal or *quartzine*. Matrix is formed by moganite-grained quartz mosaic. Vermiform microstructure is particularly typical only for zonal green ZSN (locally of "gemmy" quality) whereas it is not known from other common "silica matters" of weathered ultrabasics. The "worms" are considered to represent pseudomorphs after original chlorites, especially because of their unique structure, and mainly because the size of the vermiform aggregates reached rarely up to several centimetres. The size of individual "worms" is in most cases smaller (in the order of dozens of μm), which could indicate origin by replacement of clay minerals (smectites). Generally, vermiform aggregates are a typical and well-known structure of some chlorites and especially clay minerals, such as kaolinite, but also glauconite, known from the environment of hydrothermal alterations, terrestrial and submarine weathering, marine sedimentation, laterites and soils (Černý 1968; Tapper & Fanning 1968; Kantorowicz 1984; Wilkinson et al. 2006; Kameda et al. 2010). Gradual destruction of vermiform

Table 2: LA-ICP-MS analyses of different zones of ZSN.

Locality	Sample	ppm	B	Na	Mg	Al	K	Ca	Ti	V	Cr	Mn	Fe	Co	Ni	Sr	Ba
Přeskače	P1 core		40.2–70.8	303–446	319–2087	199–1216	188–328	116–351	17–82.9	0.28–1.16	11.1–56.6	1.39–4.29	1173–3511	1.4–11.5	10.9–93	1.43–2.73	13–62
		Mean	59	388	1195	662	272	207	47	0.6	36.2	3.2	2334	6.2	51	1.98	22
		Std dev	9	46	605	310	44	90	20	0.3	1	1	827	3.5	29	0.36	14
Přeskače	P2 margin		8.13–55.9	142–304	548–2381	405–1025	162–250	138–389	21.7–63.3	0.41–1.34	11.3–43.2	0.83–2.11	401–1178	1.42–12.8	22.3–92.2	1.82–6.50	5.17–269
		Mean	28	211	1347	697	198	272	42	0.8	26.9	1.5	703	4.8	54	2.84	45
		Std dev	22	56	616	222	34	85	14	0.3	11.8	0.5	258	3.3	25	1.44	86
Přeskače	P3 outer surface zone		LOD	119–150	2323–3297	921–1411	160–214	420–776	40–81.5	0.74–2.69	332–647	3.40–3.84	2367–3909	2.29–3.51	139–205	3.24–4.51	9.26–12.1
		Mean		134	2951	1195	182	631	62	1.5	540.2	3.6	3131	2.9	181	3.3	11
		Std dev		14	435	236	84	311	18	1	148.5	0.2	666	0.5	29	0.59	1

microstructures in cores is caused by silica recrystallization to quartz and, on the contrary, in margins and outer surface zones (rim) the replacement of "worms" and cementing by the opal-C/CT and youngest amorphous opal-A (this study, Koníčková 2014; Koníčková et al. 2015).

Accessory minerals (pyrite, barite, chlorine-rich carbonate-apatite) in cores and margins of ZSN are newly formed and not a relic mineral of serpentinite. It is therefore not only a proof of at least locally higher activity of S in fluids, but also of the reducing conditions during ZSN formation. Conditions for the formation of sulphides (pyrite) in the residues are limited to the mixing of descending meteoric waters with alkaline groundwater in the reduction zone of the weathering of serpentinites (Helvaci et al. 2017). Barite is a typical accessory mineral in marginal zones and cracks in ZSN. Barium could have a source in decomposed K-feldspar from felsic rock admixture in serpentinite and/or from the overlying marine Middle Miocene clays overlying ZSN-bearing residues in which barite is typical; dozens of localities of barite concretions from Miocene clays of the Carpathian Foredeep are known (e.g. Burkart 1953; Brzobohatý 1982).

Regional distribution

The ZSN studied, especially its zonal dark-green variety, occurs only in a very limited region of western Moravia along the eastern margin of the Gföhl Unit. It has not yet been found in numerous serpentinite localities outside this geographically restricted area elongated in the direction SW–NE between Bojanovice and Oslavany and sporadically in Waldviertel at Austria (Wanzenau). Mátl (1972) noted that the weathering-produced hydrosilicate Ni-ores in western Moravia, where the ZSN correspond distinctly to the western boundary of the Middle Miocene sediments of the Carpathian Foredeep.

Origin of zonal silica nodules (ZSN)

The origin of ZSN is related to the evolution of the paleo-weathering lateritic crusts of serpentinites. Detailed research on the mineralogy and geochemistry of these lateritic residual products has shown a rather complicated genesis in detail. Different patterns of the processes in diverse localities, affected by drainage, whole rock chemistry, removal of soluble elements, as well as wet-dry climatic changes are generally known (Freyssinet et al. 2005; Golightly 2010).

The formation of silicified zones near the surface of ultrabasics and the subsequent formation of residual rocks at most localities happened in subaeric conditions. The complete laterite profile comprises generally (from top to bottom): lateritic duricrust, plasmic (clay) zone, ferruginous saprolite, saprolite, saprock and bedrock (Samama 1986; Butt & Cluzel 2013). In the case of the plasmic zone, there is no nomenclatoric relation to the studied plasma and the mineralogical (gemological) term "plasma" is not consistent with the term plasma in pedology (Eggleton 2001). The ZNS studied are not known (published) from these profiles (e.g. Pohl 1990; Jerdysek & Halas

1990; Venturelli et al. 1997; Som & Joshi 2002; Lacinska & Styles 2013; Ulrich et al. 2014). Strong laterite-type weathering produces a saprolite with a substantial amount of dissolved SiO_2 in the upper part of the profile, which then penetrates to the base of the weathering crust (Butt & Cluzel 2013). They (especially quartz) form under the most suitable conditions close to neutral, for example, in the meteoric (low pH) and underground (high pH) water mixing zone. Strongly saturable solutions may give rise to moganite and amorphous SiO_2, which subsequently converts to opal-C/CT. The lower saturation level of the solution is suitable for the crystallization of quartz. With a gradual arrangement of the silica structure and H_2O escape, relatively slow transformations are progressing in order of amorphous opal-A → opal-CT → *chalcedony* → quartz. The *chalcedony* occurs in the incompletely filled pores of the clay residues, quartz only in opened pores. *Chalcedony* also often intimately intergrows with moganite and quartz (Lacinska & Styles 2013; Ulrich et al. 2014). Another type of alteration of ultramafics takes place under submarine conditions with typical carbonate-rich, silica-poor residues (e.g. Milliken & Morgan 1996; Silantyev et al. 2012).

In western Moravia, the residual rocks were the subject of several studies focused on similar products of laterite-like weathering, in connection with exploration for hydrosilicate Ni-ores (Kudělásek & Mátl 1971; Kudělásek et al. 1972; Mátl 1972). These original geological studies showed that weathering of lateritic type happened in the humid climate of the Tertiary but laterites with typical laterite profile which free aluminum hydroxide minerals are not developed. Silica masses were briefly mentioned from the lower parts of these profiles. The relationship between SiO_2 and MgO also influences the genesis of west Moravian ZSN. A substantial proportion of Mg from olivine and/or serpentines, eventually also Ca from clinopyroxenes and amphiboles, must have been removed during its weathering, because their silica-rich products secondary mineral assemblage is devoid of magnesite, dolomite, and sepiolite (Kudělásek & Mátl 1971; Kudělásek et al. 1972; Mátl 1972). Apart from various SiO_2 minerals, the saprolite horizon of laterite-type palaeo-weathering of serpentinites in west Moravia is composed predominantly of clay Fe–Mg alumosilicates (smectites) and chlorites. According to the relic minerals found in the ZSN, altered serpentinite is characterized by total decomposition of orthopyroxenes where Al was released while the clinopyroxenes and amphiboles remain preserved. However, unaltered ultrabasic rocks in ZSN localities are poor in Al (<1.5 wt. %) and could not serve as a source of Al. The origin of laterite residues preceded either chloritization of ultrabasics, chlorite veins or, more likely, presence of the felsic rocks near endocontacts and inside serpentinite. The influence of felsic host rocks (and their intercalations with ultrabasics) is documented by the presence of both accessory zircon and almandine among heavy minerals of saprolite, and preferential location of ZSN near the borders of serpentinite bodies (Mátl 1972; Mrázek & Rejl 1991, 2010).

Three stages of silicification and repeated silica redistribution are typical of ZSN genesis: (a) silicification of altered Al-enriched serpentinite/pure chlorite veins including their residuum which largely produced pale green/dark green silica fragments; (b) transformations of original silica to quartz, origin of zonal core-outer surface zone texture and destruction of vermiform microstructure, and (c) surface alteration up to hydrous opal or younger opal replacement and cementing of outer surface zone of already rounded ZSN.

Based on the position of various types of silica nodules in laterite-type sections of some west-Moravian localities it is possible to discuss its origin (profiles in Fig. 13).

In the bottom of profiles (bedrock), massive silica forms veins filling tectonically fractured serpentinites (Fig. 13, zone 1), see bluish-green ovals in cross-sections for specification). They have the character of white to grey to pale green coloured nodules that consist of microcrystalline quartz matrix with irregular aggregates of chlorite. The dark green type was never found here. Fragments of such homogeneous pale green nodules up to 30 cm in size were gradually disintegrated (<5–10 cm), partly rounded and are found in the whole range of the saprolite zone together with fragments of altered (chloritized) and silicified serpentinite, chiefly in the base (saprock zone). Only in localities where the saprolite zone is highly reduced due to removal of the clay-sized fraction by erosion, rounded dark green zonal nodules are common; however, chlorite–quartz–*chalcedony* fragments also appear (Fig. 13, zone 2). It is very likely that the ZSN zonality originated at a later stage during redistribution of SiO_2 in the above-mentioned "pale nodule" particles. Original chlorites were almost completely destroyed and Fe–Mg smectites dominate as a colouring component in ZSN cores (Fig. 13, zone 3). Direct replacement of clay (smectite) fraction by SiO_2 cannot be excluded, but oval-shaped ZSN have never been found inside upper clay-dominated parts of the saprolite zone (Fig. 13 – Bojanovice profile). Younger opal replaces the marginal zone of previously rounded silica fragments in the SiO_2-saturated environment.

The original weathering of serpentinite and ZNS origin in SW Moravia undoubtedly took place under terrestrial subaeric conditions, which explains their mineral associations and chemical compositions such as high SiO_2/MgO ratio, low Ca and Sr contents.

However, an open question remains, of whether the final transformations of ZSN zonality are not results of interaction with fluids of marine origin from sediments overlying serpentinite residua. The close relationship with the marine sedimentation could be suggested by the presence of barite and rare chlorine-rich "carbonate-apatite" (Koníčková 2014). However, this hypothesis needs more evidence, for example, by study of stable O and S isotopes or fluid inclusion studies.

Conclusions

The studied zonal silica nodules (ZSN), partly described as a "plasma" in gemology papers, are a characteristic component of strong Tertiary (pre-Middle Miocene in age)

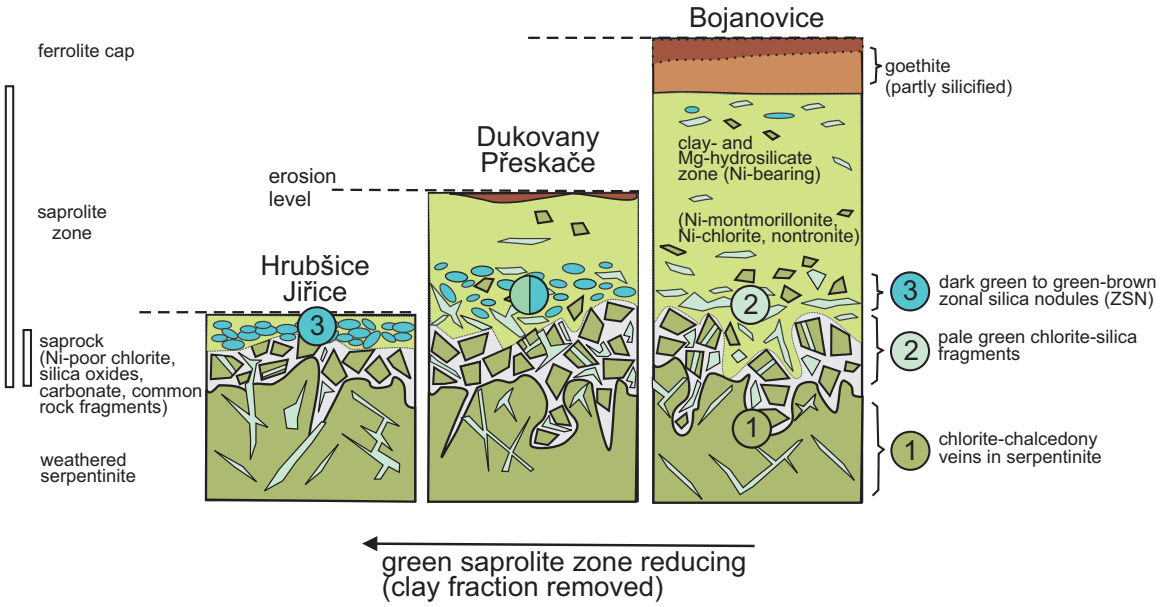

Fig. 13. Model of silica nodules distribution inside laterite-type weathering profiles from some west-Moravian localities (materials from Kudělásek et al. 1968, 1972; Mátl 1972; Samama 1986; Butt & Cluzel 2013 was used).

paleo-weathering of serpentinites and only occur in a very limited, NE–SW-oriented area of Western Moravia, Czech Republic, and sporadically in Waldviertel, Austria (both areas within the Bohemian Massif). Mineralogical studies showed that this silica variety consists predominantly of micro- and cryptocrystalline SiO_2 polymorphs with varying amounts of H_2O (quartz>>*chalcedony*>>moganite>CT/T-, and amorphous opal-A) together to finely dispersed green pigments largely of submicroscopic size (grain size in μm).

A typical feature of the ZSN studied is the concentric zonal texture: (i) microcrystalline quartz–moganite dark green "core", which is a product of complete silicification of original laterite-like residues with admixture of Fe–Mg-phyllosilicates (smectites); (ii) pale green margin shows typical opal-CT/T and vermiform microstructure in quartz matrix (±moganite, *quartzine*, *chalcedony*, with admixture of α-tridymite). This vermiform microstructure, very typical only for these ZSN, has a relic character due to the "maturation" (recrystallization) of the original gel-like SiO_2 substance; (iii) distinctly separate rim (outer surface zone) is enriched by opal.

Typical ZSN were originally products of multistage pre-Miocene paleo-weathering of serpentinites (including associated felsic rocks) in subaerial conditions. Silicification of laterite-like serpentinite residues including ZSN in the lower part of the saprolite zone took place under partial redistribution of Si–Al–Mg–Ca elements and locally at limited sulphur activity in reduced conditions in the deepest part of the profile in a pyrite stability field. Zonal silica nodules originate in the contact between strongly weathered chlorite- to clay-rich altered serpentinites (saprolite zone) and chloritized serpentinite (bedrock) in the zone of mixing of underground and descending meteoric waters. The best developed concentric zonality has rounded silica nodules from residues in which the clay-size fraction was almost removed. Typical Mg- and CO_2-poor conditions (lack of magnesite and sepiolite) are also characteristic for ZSN origin.

The regionally evident spatial relationship between ZSN and extension of the denudation relics of marine Neogene (Eggenburgian to Lower Badenian, Carpathian Foredeep) as well as restrictions of ZNS to a small area of western Moravia and adjacent Austria could indicate genetic connection. The specific zonal structure of nodules, high maturity of silica and accessory pyrite, eventually barite can support the opinion of the interaction of laterite-like residues with marine water.

Acknowledgements: The article preparation has been supported by the institutional research fund of the Faculty of Science, Masaryk University (2222/315010) to ZL and by the Ministry of Culture of the Czech Republic as part of its long-term conceptual development program for research institutions (ref. MK000094862) to SH. The authors are grateful to Markéta Holá from the Department of Chemistry, Masaryk University for LA-ICP-MS analyses, Silvestr Solnička for providing part of the plasma samples for research, Anton Beran (University of Vienna) and Jan Cempírek from our Dept. for English review of the paper and useful suggestions. We greatly thank the anonymous reviewers and editor Peter Bačík for their constructive comments, which helped to significantly improve the quality of this paper.

References

Brzobohatý R. 1982: Fish fauna of Lower Badenian calcareous clays at Brno-Královo Pole and its paleogeographical significance. *Časopis Moravského muzea*, *vědy přírodní* 67, 57–64 (in Czech).

Buchner E., Schwarz W.H., Schmieder M. & Trieloff M. 2010: Establishing a 14.6±0.2 Ma for the Nördlinger Ries impact (Germany) – A prime example for concorant isotopic ages from various dating materials. *Meteoritics & Planetary Science* 45, 662–674. https://doi.org/10.1111/j.1945-5100.2010.01046.x

Burkart E. 1953: Mährens Minerale und ihre Literatur. *Nakladatelství Československé akademie věd*, Praha, 1–1004.

Butt C.R.M. & Cluzel D. 2013: Nickel Laterite Ore Deposits. Weathered Serpentinites. *Elements* 9, 123–128. https://doi.org/10.2113/gselements.9.2.123

Černý P. 1968: Vermiform cristobalite and tridymite in siliciophites from West-Moravian serpentinites. *Časopis pro mineralogii a geologii* 13, 149–158, 173 (in Czech).

Chauviré B., Rondeau B., Mazzero F. & Ayalew D. 2017: The precious opal deposit at Wegel Tena, Ethiopia: Formation via successive pedogenesis events. *The Canadian Mineralogist* 55, 701–723. https://doi.org/10.3749/canmin.1700010

Chlupáč I., Brzobohatý R., Kovanda J. & Stráník Z. 2011: Geological history of Czech Republic. *Academia*, 1–436 (in Czech).

Dlabač M. 1976: Neogene on the southeastern edge of the Bohemian-Moravian Highlands (New researches in Moravia). *Výzkumné práce Ústředního ústavu geologického* 13, 7–21 (in Czech with English abstract).

Eggleton R.A. (Ed.) 2001: The Regolith Glossary surficial geology, soils and landscapes. *CRC for Landscape Evolution and Mineral Exploration*, Canberra, 1–144.

Francírek M. & S. Nehyba S. 2016: Evolution of the passive margin of the peripheral foreland basin: an example from the Lower Miocene Carpathian Foredeep (Czech Republic). *Geologica Carpathica* 67 41–68. https://doi.org/10.1515/geoca-2016-0003

Freyssinet P., Butt C.R.M., Morris R.C. & Piantone P. 2005: Ore-forming processes related to lateritic weathering. *Economic Geology*, 100th Anniversary Volume, 681–722. https://doi.org/10.5382/AV100.21

Golightly J.P. 2010: Progress in understanding the evolution of nickel laterites. In: Goldfarb R.J., Marsh E.E. and Monecke T. (Eds).: The challenge of finding new mineral resources – global metallogeny, innovative exploration, and new discoveries. *Society of Economic Geologists Special Publication* 15, 451–485. https://doi.org/10.5382/SP.15.2.07

Graetsch H. 1994: Structural characteristics of opaline and microcrystalline silica minerals. *Reviews in Mineralogy* 29, 209–232. https://doi.org/10.1515/9781501509698-011

Heaney P.J., Veblen D.R. & Post J.E. 1994: Structural disparities between chalcedony and macrocrystalline quartz. *American Mineralogist* 79, 452–460.

Helvaci C., Oyman T., Gündogan I., Sözbilir H., Parlak O., Kadir S. & Güven N. 2017: Mineralogy and genesis of the Ni–Co lateritic regolith deposit of the Caldag area (Manisa, western Anatolia), Turkey. *Canadian Journal of Earth Sciences* 55, 252–271. https://doi.org/10.1139/cjes-2017-0184

Hurlbut C.S. Jr. & Kammerling R.C. 1991: Gemology. 2nd ed. *John Wiley & Sons*, New York, Chichester, Brisbane, Toronto, Singapore, 1–337.

Jerdysek M.O. & Halas S. 1990: The origin of magnesite deposits from the Polish Foresudetic Block ophiolites: preliminary $\delta^{13}C$ and $\delta^{18}O$ investigations. *Terra Nova* 2, 154–159.

Kameda J., Okamoto A., Mikouchi T., Kitagawa R. & Kogure T. 2010: The occurrence and structure of vermiform chlorite. *Clay Science* 14, 155–161. https://doi.org/10.11362/jcssjclayscience.14.4_155

Kantorowicz J. 1984: The nature, origin and distribution of authigenic clay minerals from Middle Jurassic Ravenscar and Brent Group sandstones. *Clay Minerals* 19, 359–375.

Kingma K.J. & Hemley R.J. 1994: Raman spectroscopic study of microcrystalline silica. *American Mineralogist* 79, 269–273.

Koníčková Š. 2014: Occurence and mineralogy of green chalcedony (plasma) in serpentinite residues at Moravia (Moldanubian zone, Bohemian Massif). *Acta Musei Moraviae, Scientiae Geologicae* 99, 3–36 (in Czech with English abstract).

Koníčková Š., Losos Z. & Houzar S. 2015: Genesis of green plasma – specific microcrystalline silica product of serpentinite weathering (Moravian Moldanubicum, Bohemian Massif). *Bulletin mineralogicko-petrologického oddělení Národního Muzea v Praze* 23, 81–91 (in Czech with English abstract).

Kováč M., Halásová E., Hudáčková N., Holcová K., Hyžný M., Jamrich M. & Ruman A. 2018: Towards better correlation of the Central Paratethys regional time scale with the standard geological time scale of the Miocene Epoch. *Geologica Carpathica* 69, 283–300. https://doi.org/10.1515/geoca-2018-0017

Kudělásek V. & Mátl V. 1971: The serpentinites weathering crust in the south-west of Moravia. *Folia UJEP Brno* 12, 33–44 (in Czech).

Kudělásek V., Polický J. & Zamarský V. 1968: Nickel-bearing minerals of the crust of weathering of serpentinites of the area of Jamolice – Dukovany. *Sborník vědeckých prací Vysoké školy báňské v Ostravě, Řada hornicko-geologická* 14, 45–68 (in Czech).

Kudělásek V., Polický J. & Zamarský V. 1972: Mineralogic study of lateritic weathering crust of serpentinites from vicinity of Bojanovice. *Sborník vědeckých prací Vysoké školy báňské v Ostravě, Řada hornicko-geologická* 18, 73–96 (in Czech).

Kuhlemann J. 2007: Paleogeographic and paleotopographic of the Swiss and Eastern Alps since the Oligocene. *Global and Planetary Change* 58, 224–236. https://doi.org/10.1016/j.gloplacha.2007.03.007

Lacinska A. M. & Styles M. T. 2013: Silicified serpentinite – a residuum of a Tertiary paleo-weathering surface in the United Arab Emirates. *Geological Magazine* 150, 385–395. https://doi.org/10.1017/S0016756812000325

Mátl V. 1972: Deposits of hydrosilicate Ni-ores bound to the serpentinite weathering crust in southwestern Moravia. *Sborník Geologického průzkumu Ostrava* 1, 81–115.

Medaris G. Jr., Wang H., Jelínek E., Mihaljevič M. & Jakeš P. 2005: Characteristics and origins of diverse Variscan peridotites in the Gföhl Nappe, Bohemian Massif, Czech Republic. *Lithos* 82, 1–23. https://doi.org/10.1016/j.lithos.2004.12.004

Milliken K.I. & Morgan J.K. 1996: 33. chemical evidence for near-seafloor precipitation of calcite in serpentinites (site 897) and serpentinite breccias (site 899), Iberian abyssal plain. In: Whitmarsh R.B., Sawyer D.S., Klaus A. & Masson D.G. (Eds.): Proceedings of the Ocean Drilling Program. *Scientific Results* 149, 553–558.

Mrázek I. & Rejl L.1991: Gemstones of the Českomoravská vrchovina Highlands. *Muzejní a vlastivědná společnost v Brně, Západomoravské muzeum v Třebíči*, 1–135 (in Czech).

Mrázek I. & Rejl L. 2010: Gemstones of Moravia and Silesia. *Aventinum,* Praha, 1–301.

Nehyba S. & Hladilová Š. 2004: Relics of the most distal part of the Neogene foreland basin in SW Moravia. *Bulletin of Geosciences* 79, 113–120.

Novák M. 2005: Granitic pegmatites of the Bohemian Massif (Czech Republic); mineralogical, geochemical and regional classification and geological significance. *Acta Musei Moraviae, Scientiae Geologicae* 90, 3–74 (in Czech with English summary).

Pohl W. 1990: Genesis of magnesite deposits – models and trends. *Geologische Rundschau* 79, 291–299.

Pouchou J.L. & Pichoir F. 1985: "PAP" procedure for improved quantitative microanalysis. *Microbeam Analysis* 20, 104–105.

Rasser W.M., Harzhauser M., Anistratenko Y.O., Anistratenko V.V., Bassi D., Belak M., Berger J.-P., Bianchini G., Čičić S., Čosović V., Doláková N., Drobne K., Filipescu S., Gürs K., Hladilová Š.,

Hrvatović H., Jelen B., Kasiński J.R., Kováč M., Kralj P., Marjanac T., Márton E., Mietto P., Moro A., Nagymarosy A., Nebelsick H.J., Nehyba S., Ogorelec B., Oszczypko N., Pavelić D., Pavlovec R., Pavšič J., Petrová P., Piwocki M., Poljak M., Pugliese N., Redžepović R., Rifelj H., Roetzel R., Skaberne D., Sliva L., Standke G., Tunis G., Vass D., Wagreich M. & Wesselingh F. 2008: Palaeogene and Neogene. In: McCann T. (Ed.): The Geology of Central Europe. Volume 2: Mesozoic and Cenozoic. *Geological Society*, London, 1031–1140.

Rejl L., Weiss J. & Zrůstek V. 1982: Spatial distribution of metaofiolites and related rocks of the Moravian block. *Journal of Geological Sciences* 37, 137–158.

Rice S.J. & Cleveland G.B. 1955: Lateritic silicification of serpentinite in the Sierra Nevada, California. *Geological Society of America Bulletin* 66, 1660.

Samama J. 1986: Ore fields and continental weathering. *Van Nostrand Reinhold Company*, New York, 1–326.

Silantyev S.A., Novoselov A.A., Krasnova E.A., Portnyagin M.V., Hauff F. & Werner R. 2012: Silicification of Peridotites at the Stalemate Fracture Zone (Northwestern Pacific): Reconstruction of the Conditions of Low-Temperature Weathering and Tectonic Interpretation. *Petrology* 20, 21–39. https://doi.org/10.1134/S0869591112010055

Som S.K. & Joshi R. 2002: Chemical weathering of serpentinite and Ni enrichment in Fe oxide at Sukinda Area, Jajpur District, Orissa, India. *Economic Geology* 97, 165–172. https://doi.org/10.2113/GSECONGEO.97.1.165

Tapper M. & Fanning D.S. 1968: Glauconite pellets: Similar X-ray patterns from individual pellets of lobate and vermiform morphology. *Clays and Clay Minerals* 16, 275–283.

Trnka M. & Houzar S. 2002: Moldavites: a review. *Bulletin of the Czech Geological Survey* 77, 283–302.

Ulrich M., Munoz M., Guillot S., Cathelineau M., Picard Ch., Quesned B., Boulvais P. & Couteau C. 2014: Dissolution-precipitation processes governing the carbonation and silicification of the serpentinite sole of the New Caledonia ophiolite. *Contributions to Mineralogy and Petrology* 167, 952. https://doi.org/10.1007/s00410-013-0952-8

Venturelli G., Contini S. & Bonazzi A. 1997: Weathering of ultramafic rocks and element mobility at Mt. Prinzera, Northern Apennines, Italy. *Mineralogical Magazine* 61, 765–778. https://doi.org/10.1180/minmag.1997.061.409.02

Wilkinson M., Haszeldine R.S. & Fallick A.E. 2006: Jurassic and Cretaceous clays of the northern and central North Sea hydrocarbon reservoirs reviewed. *Clay Minerals* 41, 151–186. https://doi.org/10.1180/0009855064110197